Journal of Applied Physics | ARTICLE | pubs.aip.org/aip/jap

On the insignificance of dislocations in reverse bias degradation of lateral GaN-on-Si devices

Cite as: J. Appl. Phys. **135**, 025703 (2024); doi: 10.1063/5.0178743
Submitted: 28 September 2023 · Accepted: 23 December 2023 ·
Published Online: 10 January 2024

M. Stabentheiner,[1,2,a)] P. Diehle,[3] S. Hübner,[3] M. Lejoyeux,[3] F. Altmann,[3] R. Neumann,[4] A. A. Taylor,[1] D. Pogany,[2] and C. Ostermaier[1]

AFFILIATIONS

[1]Infineon Technologies Austria AG, Siemensstraße 2, 9500 Villach, Austria
[2]TU Wien, Gusshausstraße 25, 1040 Vienna, Austria
[3]Fraunhofer Institute for Microstructure of Materials and Systems IMWS, Walter-Huelse-Strasse 1, 06120 Halle, Germany
[4]Infineon Technologies Germany AG, Am Campeon 1–15, 85579 Neubiberg, Germany

[a)]**Author to whom correspondence should be addressed:** manuel.stabentheiner@infineon.com

ABSTRACT

The role of threading dislocations in the intrinsic degradation of lateral GaN devices during high reverse bias stress tests (RBSTs) is largely unknown. We now present the results on lateral p-GaN/AlGaN/2DEG heterojunctions with a width of 200 μm in GaN-on-Si. A time-dependent permanent degradation of the heterojunction under high reverse bias and elevated temperatures can be observed, ultimately leading to a hard breakdown and device destruction. By using an integrated series p-GaN resistor, the device is protected from destruction and, consequently, the influence of dislocations on the degradation mechanism could be studied. Localization by emission microscopy could show that the transient current increase during a RBST is the result of the creation of a limited amount of highly localized leakage paths along the whole device width. We could establish a 1:1 correlation of leakage sites with a structural material degradation within the AlGaN barrier for nine individual positions on two different devices by planar transmission electron microscopy analysis. To unambiguously show whether dislocations in GaN-on-Si even should be considered a potential trigger for the RBST degradation in lateral heterojunctions, a combined planar and cross-sectional lamella approach was used for the first time for larger devices. This enabled the visualization of the three-dimensional propagation path of the dislocations close to the degradation sites. It was found that there is no statistically significant link between the material degradation and pre-existing dislocations. Our findings offer new insights into the GaN-on-Si material system, upon which upcoming power technologies are built upon.

Published under an exclusive license by AIP Publishing. https://doi.org/10.1063/5.0178743

I. INTRODUCTION

In the recent years, the wide bandgap material GaN has been used not only in optoelectronics, but is also making an advance into the power semiconductor market. GaN power devices are typically grown on a silicon substrate to lower the costs.[1] However, the large lattice mismatch between GaN and Si introduces a very high amount of threading dislocations (TDs) in the order of $1–6 \times 10^9\,\text{cm}^{-2}$.[2]

To this day, only little is known about the electrical properties of these crystal defects, especially at higher voltages. Conductive-AFM studies on GaN-on-Si imply that mostly dislocations with a screw-component are electrically active.[3] However, these studies are always limited to voltages below 10 V and it is hard to draw a conclusion about how TDs would behave electrically under real operating conditions in a macroscopic device. While the influence of dislocations on device parameters and device degradation has been extensively studied in GaN-on-GaN PN diodes,[4–7] there are almost no data available for GaN-on-Si HEMTs. Whereas an influence of TDs on the vertical breakdown[8] and gate failure[9] of HEMTs is, in some cases, implied, a direct correlation is never shown.

Linking electrical behavior and localized leakage paths from a large-scale device with microscopic crystal defects is a challenging task.[10] Thereby, the physical limitations of standard failure analysis flows and localization methods are key reasons why a direct correlation between TDs and material degradation in GaN-on-Si devices is rarely seen in the literature and a correlation can only be implied.

Published under an exclusive license by AIP Publishing

Emission microscopy (EMMI) is a commonly used non-invasive method for localizing leakage paths under specific bias conditions.[11] EMMI is capable of detecting defect-related emissions, but the resolution of this optical analysis technique is constrained by the detected wavelength and the quality of the optics used. The resulting inaccuracies, paired with the high risk of cutting away parts of the defect in a standard cross-sectional lamella with a thickness of 100–400 nm, significantly lower the chances of identifying the real failure cause.

As mostly GaN-on-Si HEMTs with a p-GaN gate technology are used in the industry, the reliability of the lateral p-GaN/AlGaN/2DEG heterojunction is of key interest. Several studies on Schottky HEMTs have shown that devices can experience time-dependent lateral degradation when they are submitted to long-term reverse bias stress; even at a stress bias that is significantly lower than the breakdown voltage.[12–14] Bajo *et al.* already showed that the occurrence of emission spots along the device width can be directly correlated with a leakage current increase during stress.[15] It was also shown by Bajo *et al.*[15] and Sun *et al.*[16] that the current at each leakage path eventually converges and the degradation of the device saturates after the maximum number of leakage sites is reached. However, no reports showing spot emission in a p-GaN HEMT as a result of stress have been published so far. A previous study on tailored sub-micrometer p-GaN/AlGaN/uid-GaN test structures could find first indications that the intrinsic material degradation under reverse bias stress tests (RBSTs) is independent of TDs.[17] In that study, damage within the AlGaN barrier was induced close to an intended position at a sharp tip electrode with a high and inhomogeneous electric field. However, from these findings, it remains difficult to draw conclusions on the role of TDs within a large-scale device with a more uniform electric field distribution.

This study aims to clarify whether dislocations in GaN-on-Si even should be considered a potential trigger for the RBST degradation in lateral heterojunctions with larger device widths. In contrast to sub-micrometer devices, in which no localization is necessary, we tackle the problem of limited localization accuracy related to emission microscopy. By combining EMMI localization on 200 μm wide test devices with an advanced microstructural characterization workflow, we could find a clear correlation between the intrinsic material degradation and leakage paths that evolved during the RBST. The applied analysis approach was found to be essential to clearly show that there is no statistically significant link between degradation sites and pre-existing dislocations.

II. EXPERIMENTAL METHODS

The samples used in this study were grown by metalorganic chemical vapor deposition (MOCVD) on a 6 in. silicon substrate. The device under test (DUT) consists of a lateral p-GaN/AlGaN/uid-GaN heterostructure [Fig. 1(a)]. The thickness of the p-GaN, AlGaN (~17% Al content), and uid-GaN is 200, 80, and 150 nm, respectively. The 2DEG, which is formed at the interface of the uid-GaN and the AlGaN layer, connects the heterojunction electrically with a contact located 2 μm away from the p-GaN. The surface is passivated by a SiN layer. If a reverse bias is applied between the ohmic contact on the p-GaN and the 2DEG contact, then the 2DEG is laterally depleted and the point of the highest electric field is located directly at the p-GaN corner. Intentionally, no field plate was implemented above the heterojunction, although this would have had a positive effect on the electric field reduction. Consequently, this enabled spatially resolved localization of leakage paths by EMMI from the frontside.

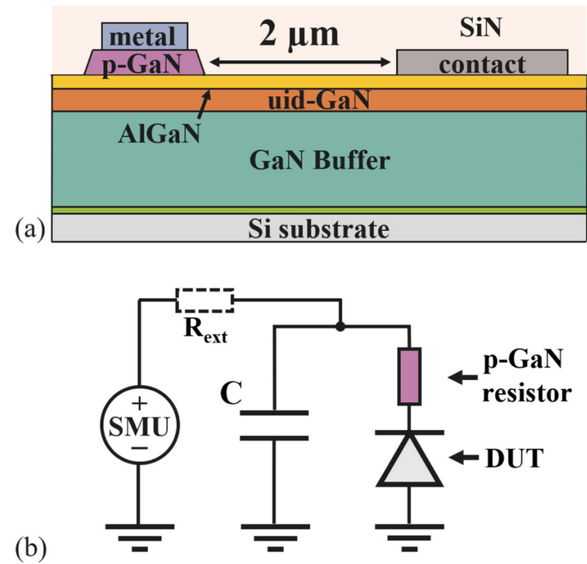

FIG. 1. (a) Schematic cross section of the device under test (DUT). The lateral PIN (p-GaN/AlGaN/2DEG) heterojunction extends over a device width of 200 μm. (b) Circuit representation of the measurement chain. An on-chip high-ohmic p-GaN resistor is integrated in series to the DUT.

The DUT extends over a width of 200 μm and has a static breakdown voltage of ~310 V. Similar to a previous study,[17] a p-GaN resistor with a resistance of ~1.6 MΩ is integrated next to the DUT, as indicated in the circuit diagram in Fig. 1(b). Typically, if only an external limiting resistor [R_{ext} in Fig. 1(b)] is used, the energy stored in the external (cables, printed circuit boards, etc.) (and internal) capacitances [C in Fig. 1(b)] would lead to large meltdowns in the case of a hard failure, thereby rendering a meaningful physical analysis of the failure site impossible. However, the integrated series resistor effectively acts as a current limiter and, furthermore, as a voltage divider and will protect the device from destruction.

IV and RBST measurements shown in this study were performed on a Keithley 2634B Source Measure Unit (SMU) under a controlled chuck temperature of 150 °C. For EMMI frontside localization, a Phemos-1000 microscope by Hamamatsu Photonics equipped with a Si-CCD camera with a wavelength sensitivity between 400 and 1200 nm was used. For the purpose of the physical failure analysis of stressed devices, planar samples of the region of interest were prepared by first laser (microPREP™), followed by plasma and gallium focused ion beam (FIB) milling. Cross-sectional lamellas were prepared by gallium FIB milling and *in situ* lift out technique. More details on the applied preparation

Published under an exclusive license by AIP Publishing

workflow can be found in the supplementary material and elsewhere.[17,18] Scanning-TEM (STEM) images were taken with a 300 kV aberration corrected FEI Titan[3] G2 60-300.

III. RESULTS AND DISCUSSION

A. Electrical measurements

Figure 2(a) displays the results of reverse bias stress tests (RBSTs) conducted at 180 V at a temperature of 150 °C on seven devices, two of which were tested with a series resistor and five without. These conditions were chosen so that the degradation occurs within a time window of 100 and 1000 s. It can be seen in Fig. 2(a) that all devices experience a time-dependent degradation after ∼60 s. The degradation shares similarities to studies on HEMT structures.[14] The noisy signal after the onset of the degradation indicates the creation of defects that form a percolation path within the device.[15,19] The time-to-breakdown lies within a narrow time window at around 100 s, indicating that the degradation and

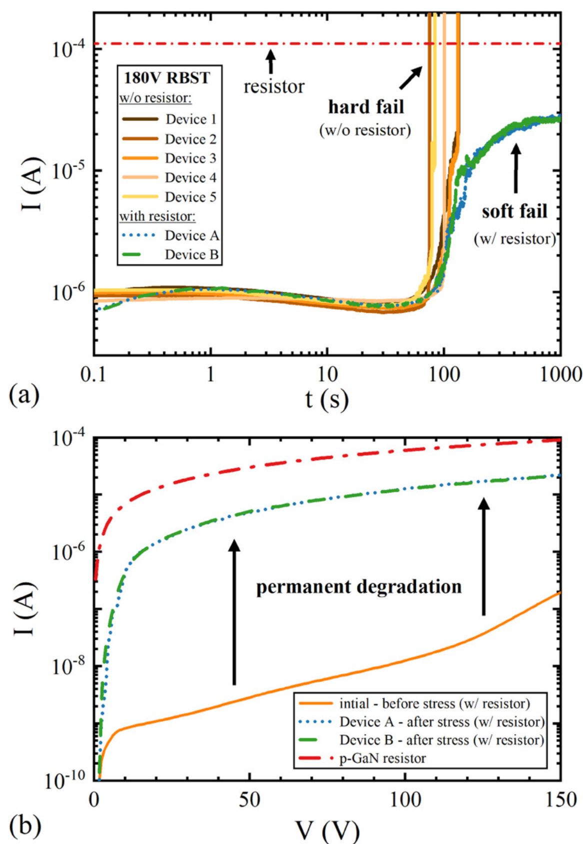

FIG. 2. (a) Evolution of current under reverse bias stress tests (RBSTs) at 180 V and 150 °C. Devices 1–5 without any protection experience a hard fail, while device A and device B with a series safety resistor exhibit a soft failure and stabilize after 1000 s. (b) IV characteristics of Device A and Device B at 150 °C showing permanent degradation and ohmic behavior after the RBST.

the breakdown are of intrinsic nature and not related to processing variations. Such a narrow distribution of time-to-breakdown, indicating intrinsic failure mode, has also been observed in p-GaN structures with intentional degradation at the position of a sharp tip.[17] All tested devices without a series resistor in Fig. 2(a) experience a hard fail shortly after the onset of the degradation. This causes in all cases a large meltdown at the laterally confined failure position and prohibits any meaningful physical failure analysis. A highly localized current flow may lead to a thermal runaway and a burnout.

On the other hand, the use of the series resistor is shown to effectively prevent a hard fail of the device [see device A and device B in Fig. 2(a)], thus leading to a soft failure. However, the time-to-breakdown is not affected by the use of the series resistor. The soft failure is explained by the reduction in the stress voltage at the heterojunction V_{DUT} during the degradation by using a simple voltage divider formula, with V_{SMU} being the applied stress voltage, R being the resistance of the safety resistor, and $I(t)$ being the measured current over time,

$$V_{DUT}(t) = V_{SMU} - R^{*}I(t). \tag{1}$$

At the start of the stress, V_{DUT} is ∼178 V and almost as high as V_{SMU}. Once the degradation starts, V_{DUT} gradually decreases. Consequently, at the end of the stress test at 1000 s, V_{DUT} has been reduced to ∼135 V with a current of $\sim 3 \times 10^{-5}$ A. This current is lower than the limit imposed by the series resistor [see Fig. 2(a)], indicating that the damage between the p-GaN and the channel is not a perfect short and/or that it is strongly localized so the current flows just via a part of the device width. This softening of the stress condition over time prevents that the critical stress limit at a single position is exceeded and a meltdown can occur. The transient current reaches a plateau after 1000 s after which no further degradation is noticeable. Similar behavior has been observed in other studies on Schottky HEMTs even without the use of a series resistor.[16,20] The results suggest that the degradation mechanism of p-GaN heterojunctions under RBST could be closely related to the degradation observed on Schottky HEMTs, with the presence of an AlGaN barrier as the common feature. The IV characteristic of both devices (with the p-GaN resistor still being connected) in Fig. 2(b) clearly shows that after stress, the current is permanently degraded by 2–4 orders of magnitude over the measured voltage range. The comparison to the IV curve of the series resistor indicates the presence of ohmic leakage paths within the reverse-biased heterojunction.

B. Failure localization by EMMI

Figure 3 depicts the EMMI images of Device A and Device B, taken at 100 V and ambient temperatures after permanent degradation occurred. During the EMMI measurement, both devices displayed a current of about 3 μA. The chosen imaging and bias conditions were found to be ideal from the point of view of the detected EMMI spot size, emission intensity, and integration time (higher currents would only cause unnecessary enlargement of EMMI spots). In the top panels of Figs. 3(a) and 3(b), it can be seen that around 30 highly localized emission spots have evolved on both devices along the 200 μm device width. The superposition

Published under an exclusive license by AIP Publishing

of many degrading leakage paths explains the smoother current transient seen in Fig. 2(a) compared to small scale devices with only one degradation site, which show a much noisier transient.[17] The emission has its highest intensity at the reverse-biased p-GaN/AlGaN/2DEG heterojunction, meaning that the defect can be expected near the p-GaN corner [see Fig. 1(a)]. For the devices tested without a series resistor, it is assumed that they failed if the current flow at one of those evolving leakage positions exceeded a certain current limit. The detailed images of the EMMI localization show the five spots labeled A–E for Device A [Fig. 3(a)] and the four spots labeled 1–4 for Device B [Fig. 3(b)], which have been chosen for further analysis.

C. Physical failure analysis

The EMMI spot size seen in Fig. 3 is about 1 μm in diameter, which is generally not accurate enough to pinpoint a failure signature to a single crystal defect with the expected dislocation densities of 4×10^9 cm^{-2} (=40 μm^{-2}) in GaN-on-Si.[17] Additional measurement errors can also occur during or between the localization and the subsequent failure analysis steps, e.g., by overlay calibration errors between CCD scanning and emission images, and differences in the magnification calibration of different tools and in sample orientation. In summary, a small error in localization or in the subsequent failure analysis steps can already mean that a completely different position (and in this case, dislocation) is suspected of being the cause of the emission spot. This highlights the importance of the thorough analysis workflow that we applied in this study. Therefore, we have chosen a combined planar and cross-sectional lamella approach for the physical failure analysis to overcome the described limitations of localization accuracy (Fig. 4).

To enable the correlation between EMMI localization and physical analysis, we milled holes with the FIB next to the positions of the emission spots after correlating EMMI and scanning electron microscopy (SEM) images, which later served as a reference point. In the first part of the TEM investigation, a planar lamella with a thickness of about 600 nm was prepared at both Device A and Device B and was investigated by STEM [Fig. 4(b)]. A planar TEM lamella enables not only the analysis of multiple defect sites at the same time but also the visualization of all crystal defects in proximity of the failure position. Measuring the distances of the spots along the width relative to a reference point enables later identification of the positions within the TEM analysis. During TEM analysis, an offset between the position of the reference markers and the defects up to 400 nm was observed. This illustrates well the previously mentioned correlation challenges and why a planar preparation at the beginning is advantageous.

At each of the nine inspected emission spots visible in Fig. 3, a structural degradation, seen as a darker area marked with red arrows in Figs. 5(a) and 6(a), was observed close to the p-GaN

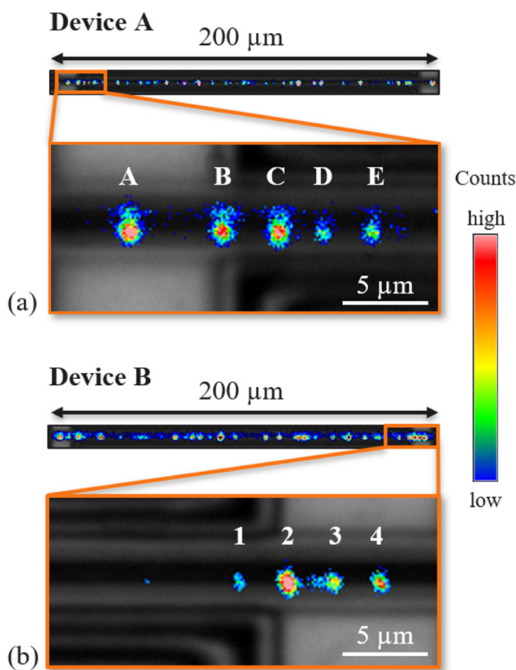

FIG. 3. EMMI image of devices with a series resistor at a reverse bias of 100 V. Multiple leakage paths are visible as emission spots along the 200 μm device width. The nine spots that have been chosen for further STEM investigation are shown in the detailed images. (a) Device A with five spots labeled A–E. (b) Device B with four spots labeled 1–4.

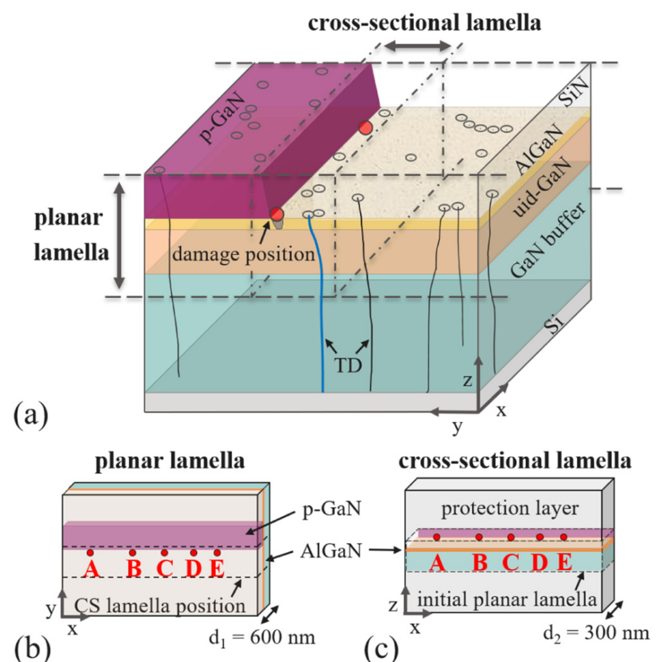

FIG. 4. Schematics of the structure and the respective lamella geometries. (a) 3D visualization of the lateral heterojunction in respect to the lamella volumes. Examples of degradation sites at the p-GaN corner and TDs are indicated with red circles and lines, respectively. Planar (b) and cross-sectional lamella (c) including EMMI spots A–E.

Published under an exclusive license by AIP Publishing

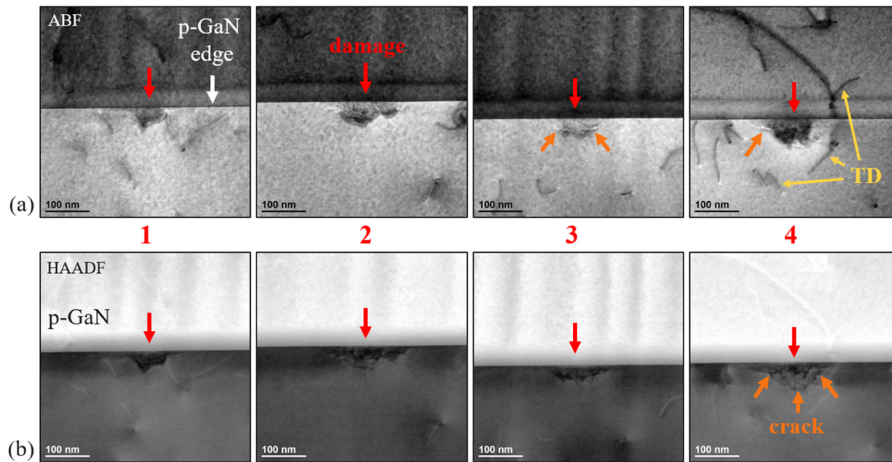

FIG. 5. STEM images of the planar lamella including EMMI spots 1–4 of Device B. A structural degradation in the AlGaN barrier can be seen at every EMMI spot position. (a) Dislocations (TDs) are visible as lines in the annular bright-field (ABF) detector signal; (b) small cracks and the full extent of the structural damage can be clearly identified in the high-angle annular dark-field (HAADF) detector signal.

edge. A 1:1 correlation of damage within the AlGaN barrier next to the p-GaN edge and EMMI spot positions could be established for both Device A and Device B. Within the STEM images, TDs are better visible in the annular bright-field (ABF) signal, since it is more sensitive to diffraction contrast. However, the damage in the AlGaN barrier can be seen more clearly in the high-angle annular dark-field (HAADF) signal of device B [Fig. 5(b)]. Small cracks and other signs of structural degradation be clearly identified within the AlGaN barrier. The p-GaN on the other hand appears to be undamaged. In the past, the appearance of cracks along the gate of a HEMT structure has been associated with high power stress and drain current degradation.[21,22] In some cases, pitting within the AlGaN barrier was reported at the failure sites of devices stressed under reverse bias.[20] A clear answer on why pits developed in the AlGaN barrier was not found, and a hypothesis on the involvement of TDs was formulated but not proven.[15] All the previous studies have in common that the highest electric field (and the damage or emission) is located at the drain-sided edge of the gate.

While some defect areas [like positions 2 and 3 in Fig. 5(a)] do not seem to be associated with a TD, for others the interpretation remains more difficult. From the top-view perspective, the structural damage could cover a dislocation that lies below due to projection. For this reason, in a second step, a ∼300 nm thick cross-sectional lamella parallel to the p-GaN edge has been prepared from the planar lamella of device A as illustrated in Figs. 4(a)–4(c). To answer the question, if a dislocation is inside the

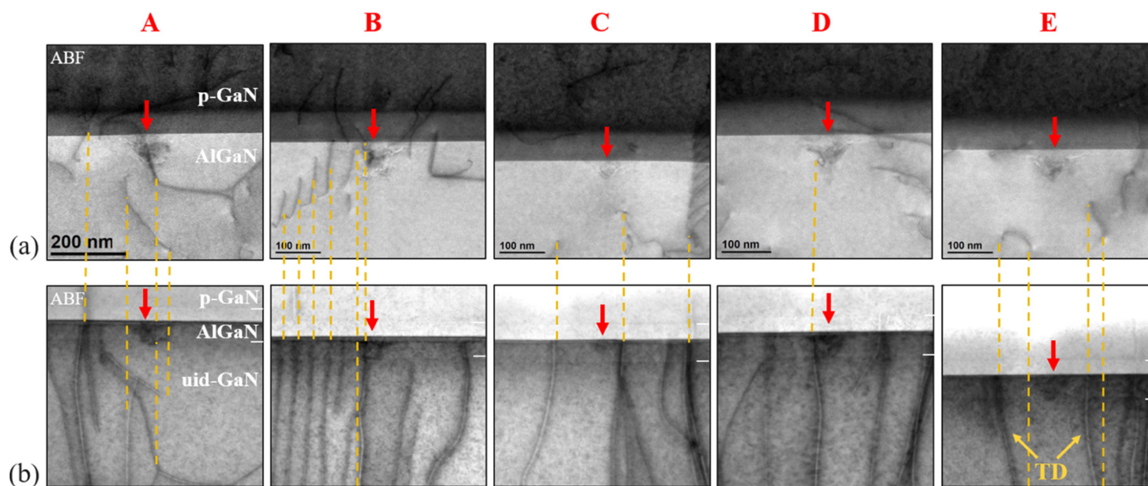

FIG. 6. Combined planar and cross-sectional TEM approach on Device A. (a) ABF STEM top-view images of the planar lamella at each leakage spot position. (b) Corresponding ABF STEM images showing the cross-sectional view. Yellow dashed lines between (a) and (b) correlate the dislocations. The three-dimensional propagation of the dislocations relative to the defect sites can now be seen. Damages in the AlGaN barrier reach the 2DEG. Only two out of five defect sites (B and D) align with a dislocation.

Published under an exclusive license by AIP Publishing

degraded volume, the investigation of two orthogonal perspectives is required.[17] The applied method represents the only way to exclude overlapping effects due to 2D projection and to preserve all dislocations near the failure site.

As illustrated in Fig. 6, each dislocation visible in the top-view images could be visualized in the cross-sectional lamella. The degradation is found to be confined to the AlGaN barrier layer. The damage reaches the AlGaN/uid-GaN at spot positions A, B, D, and E, likely forming a direct leakage path through the AlGaN barrier. The observed structural damage is in good agreement with the failure signature found in smaller devices under similar test conditions.[17] In three out of five degradation sites (spot positions A, C, and E), it is evident that the failure sites and the structural damages do not correlate with dislocations.

Position A [first panel in Figs. 6(a) and 6(b)] demonstrates well why only a planar view image could be misleading. While from the top, it looks like a TD, which is directly leading to the damage site, the cross-sectional view below shows that the path of the TD is far below the AlGaN barrier. Similarly, looking only at position C in the cross-sectional image, one assumes that a bundle of dislocations is in close proximity to the damage, while it is evident in the planar image that they are 100 nm away and not related. The pathway of the TD close to the degradation site C is schematically drawn and highlighted in blue in Fig. 4(a). In positions B and D, a dislocation could be identified, which is running through or is close to a degradation site. Considering a defect area with a diameter of 100 nm and a TD density of $4 \times 10^9\,\mathrm{cm}^{-2}$, about two out of five defect areas should contain a TD. This fits the observation of a TD at spots B and D, further underlining that there is no statistically significant link. Whether these two dislocations are actually electrically active or not cannot be determined.

D. Discussion

Based solely on the observed damage diameter of approximately 100 nm and the given TD density, it can be estimated that there are a total of 800 TDs close to the p-GaN edge along the 200 μm device width. The amount of conductive TDs within an AlGaN barrier (under forward bias conditions) has been observed by Besendörfer *et al.*[3] to strongly depend on the growth parameters and the crystal quality, ranging from 0.8% up to 4.8% of the total TD density. The high variation between samples already indicates that each sample has to be seen as an individual and comparisons with reported studies on different epitaxial stacks are highly questionable. Furthermore, it has not been shown that TDs that are electrically active under low forward bias are also electrically active under high reverse bias conditions.

Unfortunately, the density of conductive dislocations on our samples is unknown for both forward and reverse bias. Nonetheless, if there would be a link between emission spots and conductive dislocations, then the presence of about 30 emission spots along the devices would result in ∼3.8% of all TDs at the corner being electrically active. A percentage of 3.8% theoretically lies within the reported range of conductive TD densities. However, it becomes clear that a link with TDs could only be implied, if certain assumptions about both the density and the electrical relevance of TDs under the applied bias conditions are made. If dislocations would be the main defect type responsible for intrinsic material degradation of the AlGaN barrier in an RBST, one would expect that all investigated degradation sites localized by EMMI can be clearly correlated to TDs, since there are more TDs present within 100 nm of the p-GaN edge than observed emission spots. It is also not a priori clear, whether the dislocations, which appears conductive in a C-AFM study of epitaxial material,[3] will be electrically active in a processed sample. Vice versa, inactive dislocation in the epi-material could become activated during the fabrication process. These aspects are objects of further studies. Our applied analysis approach, however, provides clear evidence that lateral heterojunctions can degrade at a seemingly random position, regardless of the presence of threading dislocations.

Based on the findings, we can start a discussion about the potential degradation mechanism. Each investigated spot position showed the same failure signature with cracks and pitting in the AlGaN barrier layer. An electrochemical reaction was proposed in Ref. 20. However, the samples are passivated with a thick SiN layer, which should strongly suppress the diffusion of impurities toward the p-GaN edge. A native oxide layer can still always be present.[23] While we also see that the degradation saturates, this can also be related to the use of the safety resistor, which lowers the stress voltage, and not due to the formation of an exclusion zone due to the depletion of mobile species.[20]

In any case, the degradation mechanism would require spatial inhomogeneities in the leakage current and/or the electric field along the device width to form local degradation sites. This could be caused, e.g., by local differences in the etching process that lead to small differences in the geometry of the edge. However, those variations seem to have only a small influence on the time-to-breakdown. The inhomogeneity just leads to the formation of a degradation spot at this preferred position. It is beyond the scope of this paper to discuss what should be a minimum size of such an inhomogeneity so that the spot forms at its position.

A link between electrical degradation and defect formation as a result of the stress associated with the piezoelectric effect has been postulated in the past.[24,25] Even without any bias applied, the AlGaN barrier is already under tensile strain due to the lattice mismatch between AlGaN and GaN. On top of that, the piezoelectric effect could further strain and weaken the bonds under the high electric field present at the p-GaN edge and create crystallographic defects if the stored elastic energy exceeds a critical limit.[25] The lower estimate of the electric field under used stress conditions, considering a homogeneous electrical field between the electrodes, is ∼1 MV/cm. However, the electric field at the p-GaN edge might be much higher due to corner effects.

Additionally, free charge carriers created by, e.g., band-to-band tunneling, could locally recombine and enhance defect reactions by releasing energy,[26] thereby bringing the elastic energy over the critical limit and aiding the creation of defects. Over time, once defect orbitals start to overlap, a percolation path toward the 2DEG forms, hence leading to a noisy signal and an increased current flow at that position.[22] The localized current flow can further enhance the material degradation during stress until larger cracks and pits develop.

To significantly delay the onset of the intrinsic degradation, it is recommended to lower the electric field at the edge of the

Published under an exclusive license by AIP Publishing

p-GaN. By lowering the electric field, the intrinsic leakage current component caused by band-to-band tunneling is also lowered. That can be accomplished, for example, through the integration of field plates.

VI. CONCLUSIONS

In conclusion, the intrinsic material degradation of lateral heterojunctions in GaN-on-Si under high reverse bias stress tests (RBSTs) was studied. The time-to-breakdown lies within a narrow time window and indicates that the electrical failure is intrinsic and not extrinsic. The use of a series p-GaN resistor helped to protect the device from a hard fail, leading to the formation of multiple leakage paths along the whole device width, which were visualized with emission microscopy. A highly localized permanent structural degradation of the AlGaN barrier was revealed to be the failure signature. After looking at nine individual leakage positions, a 1:1 correlation between located emission spots after degradation and crystallographic damage in the AlGaN barrier was found by planar STEM analysis.

We have shown that the used combined planar and cross-sectional TEM approach, applied previously on sub-micrometer devices,[17] can be successfully applied for HEMT-like structures used in this work. This combined TEM approach has offered an understanding of the three-dimensional pathway of dislocations at multiple defect sites. The investigation could successfully show that the degradation of lateral p-GaN/AlGaN/2DEG heterojunctions under high reverse bias is not 100% linked with the presence of pre-existing dislocations. Spatial inhomogeneities in both the electric field and the leakage current are suspected to be the trigger for this degradation mode. A similar analysis approach can be used for other stress conditions to further exclude dislocations as reliability relevant defects in GaN-on-Si.

SUPPLEMENTARY MATERIAL

See the supplementary material for details on the applied preparation workflow (Figs. S1 and S2). The high number of dislocations near the p-GaN edge can be seen in a stitched STEM overview image of the surrounding area of spot B on Device A (Fig. S3). The complementary HAADF STEM top-view images of the planar lamella on device A at each leakage spot position are shown in Fig. S4.

ACKNOWLEDGMENTS

M. Stabentheiner, P. Diehle, S. Hübner, M. Lejoyeux, F. Altmann, A.A. Taylor, and C. Ostermaier received funding from the ECSEL Joint Undertaking (JU) under Grant Agreement No. 826392. The JU receives support from the European Union's Horizon 2020 research and innovation program and Austria, Belgium, Germany, Italy, Slovakia, Spain, Sweden, Norway, and Switzerland.

AUTHOR DECLARATIONS

Conflict of Interest

The authors have no conflicts to disclose.

Author Contributions

M. Stabentheiner: Conceptualization (lead); Investigation (equal); Methodology (equal); Visualization (lead); Writing – original draft (lead); Writing – review & editing (equal). **P. Diehle:** Investigation (equal); Methodology (equal); Writing – review & editing (equal). **S. Hübner:** Investigation (supporting). **M. Lejoyeux:** Investigation (supporting). **F. Altmann:** Writing – review & editing (supporting). **R. Neumann:** Investigation (supporting). **A. A. Taylor:** Methodology (supporting). **D. Pogany:** Supervision (equal); Writing – review & editing (equal). **C. Ostermaier:** Supervision (equal).

DATA AVAILABILITY

The data that support the findings of this study are available from the corresponding author upon reasonable request.

REFERENCES

[1]H. Amano *et al.*, "The 2018 GaN power electronics roadmap," J. Phys. Appl. Phys. **51**(16), 163001 (2018).
[2]H. Marchand *et al.*, "Metalorganic chemical vapor deposition of GaN on Si (111): Stress control and application to field-effect transistors," J. Appl. Phys. **89**(12), 7846–7851 (2001).
[3]S. Besendörfer, "Statistical investigation of dislocation induced leakage current paths in AlGaN/GaN HEMT structures on Si and the impact of growth conditions," Appl. Phys. Express **15**, 095502 (2022).
[4]H. Ohta, N. Asai, F. Horikiri, Y. Narita, T. Yoshida, and T. Mishima, "Impact of threading dislocations in GaN p–n diodes on forward I–V characteristics," Jpn. J. Appl. Phys. **59**(10), 106503 (2020).
[5]H. Ohta, N. Asai, F. Horikiri, Y. Narita, T. Yoshida, and T. Mishima, "Breakdown phenomenon dependences on the number and positions of threading dislocations in vertical p-n junction GaN diodes," Jpn. J. Appl. Phys. **60**(SB), SBBD09 (2021).
[6]S. Usami *et al.*, "Correlation between dislocations and leakage current of p-n diodes on a free-standing GaN substrate," Appl. Phys. Lett. **112**(18), 182106 (2018).
[7]T. Narita *et al.*, "Identification of type of threading dislocation causing reverse leakage in GaN p–n junctions after continuous forward current stress," Sci. Rep. **12**(1), 1458 (2022).
[8]M. Borga *et al.*, "Evidence of time-dependent vertical breakdown in GaN-on-Si HEMTs," IEEE Trans. Electron Devices **64**(9), 3616–3621 (2017).
[9]S. Besendörfer, E. Meissner, F. Medjdoub, J. Derluyn, J. Friedrich, and T. Erlbacher, "The impact of dislocations on AlGaN/GaN Schottky diodes and on gate failure of high electron mobility transistors," Sci. Rep. **10**(1), 17252 (2020).
[10]D. A. Cullen *et al.*, "Electroluminescence and transmission electron microscopy characterization of reverse-biased AlGaN/GaN devices," IEEE Trans. Device Mater. Reliab. **13**(1), 126–135 (2013).
[11]N. Moultif, A. Divay, E. Joubert, and O. Latry, "Localizing and analyzing defects in AlGaN/GaN HEMT using photon emission spectral signatures," Eng. Failure Anal. **81**, 69–78 (2017).
[12]M. Meneghini *et al.*, "Extensive investigation of time-dependent breakdown of GaN-HEMTs submitted to OFF-state stress," IEEE Trans. Electron Devices **62**(8), 2549–2554 (2015).
[13]M. Meneghini *et al.*, "Electroluminescence analysis of time-dependent reverse-bias degradation of HEMTs: A complete model," in *2011 International Electron Devices Meeting* (IEEE, 2011), pp. 19.5.1–19.5.4.
[14]G. Meneghesso *et al.*, "Degradation of AlGaN/GaN HEMT devices: Role of reverse-bias and hot electron stress," Microelectron. Eng. **109**, 257–261 (2013).

Published under an exclusive license by AIP Publishing

[15]M. Montes Bajo, C. Hodges, M. J. Uren, and M. Kuball, "On the link between electroluminescence, gate current leakage, and surface defects in AlGaN/GaN high electron mobility transistors upon off-state stress," Appl. Phys. Lett. **101**(3), 033508 (2012).

[16]H. Sun, M. Montes Bajo, M. J. Uren, and M. Kuball, "Implications of gate-edge electric field in AlGaN/GaN high electron mobility transistors during OFF-state degradation," Microelectron. Reliab. **54**(12), 2650–2655 (2014).

[17]M. Stabentheiner *et al.*, "Test concept for a direct correlation between dislocations and the intrinsic degradation of lateral PIN diodes in GaN-on-Si under reverse bias," Microelectron. Reliab. **150**, 115071 (2023).

[18]M. Simon-Najasek, S. Huebner, F. Altmann, and A. Graff, "Advanced FIB sample preparation techniques for high resolution TEM investigations of HEMT structures," Microelectron. Reliab. **54**(9–10), 1785–1789 (2014).

[19]M. Meneghini *et al.*, "Time-dependent degradation of AlGaN/GaN high electron mobility transistors under reverse bias," Appl. Phys. Lett. **100**(3), 033505 (2012).

[20]M. M. Bajo, H. Sun, M. J. Uren, and M. Kuball, "Time evolution of off-state degradation of AlGaN/GaN high electron mobility transistors," Appl. Phys. Lett. **104**(22), 223506 (2014).

[21]U. Chowdhury *et al.*, "TEM observation of crack- and pit-shaped defects in electrically degraded GaN HEMTs," IEEE Electron Device Lett. **29**(10), 1098–1100 (2008).

[22]D. Marcon *et al.*, "Reliability analysis of permanent degradations on AlGaN/GaN HEMTs," IEEE Trans. Electron Devices **60**(10), 3132–3141 (2013).

[23]F. Gao *et al.*, "Role of oxygen in the OFF-state degradation of AlGaN/GaN high electron mobility transistors," Appl. Phys. Lett. **99**(22), 223506 (2011).

[24]J. Joh and J. A. del Alamo, "Mechanisms for electrical degradation of GaN high-electron mobility transistors," in *2006 International Electron Devices Meeting* (IEEE, San Francisco, CA, 2006), pp. 1–4.

[25]J. A. del Alamo and J. Joh, "GaN HEMT reliability," Microelectron. Reliab. **49**(9–11), 1200–1206 (2009).

[26]L. C. Kimerling, "Recombination enhanced defect reactions," Solid-State Electron. **21**(11), 1391–1401 (1978).

Published under an exclusive license by AIP Publishing